Met. Mater. Int., Vol. 21, No. 5 (2015), pp. 956~961
doi: 10.1007/s12540-015-4443-5

Growth and Structure of Mg-Al Spinel Nanodonut-Decorated MgO Nanowires

Yong Jung Kwon[1], Han Gil Na[1], Sang Sub Kim[2,*], Ping Wu[3], and Hyoun Woo Kim[1,*]

[1]Division of Materials Science and Engineering, Hanyang University, Seoul 133-791, Republic of Korea
[2]Department of Materials Science and Engineering, Inha University, Incheon 402-751, Republic of Korea
[3]Entropic Interface Group, Singapore University of Technology & Design, Singapore 138682, Singapore

(received date: 25 September 2014 / accepted date: 4 June 2015)

We report the growth of MgO nanowires surrounded by a donut-shaped spinel in a periodic way at a particular growth temperature of 1,000 ℃. We examined the samples by means of scanning electron microscopy, transmission electron microscopy, selected area electron diffraction, and X-ray diffraction. At a lower temperature 950 ℃, regular MgO nanowires grow. In contrast, at a higher temperature of 1,050 ℃, spinel of $(Mg_{0.4}Al_{0.6})Al_{1.8}O_4$ nanowires grow. From the absence of tip nanoparticles, we suggest that the synthesis of nanowires in the present study is dominated by a base-growth process. Based on the thermochemistry calculations, we propose that the absence of spinel in samples equilibrated at 950 ℃ is due to the catalytic-like behaviors of the silicon substrate which promotes the formation of MgO. In terms of choosing appropriate source materials, the technique reported here can be extended and exploited to produce various combinations of nanowire backbone structure with a surrounded nano-scale disk.

Keywords: composites, fibers, chemical synthesis, scanning electron microscopy (SEM), transmission electron microscopy (TEM)

1. INTRODUCTION

As a useful ceramic material, magnesium aluminate spinels have a variety of applications including vis-UV transparent domes, windows and lamp envelopes [1-3], catalyst support [4,5], nuclear waste management [6], armor [7], humidity sensors [8] and bonding agents in cement castables [9].

With spinel being the only ternary compound in the MgO/Al_2O_3 phase diagram, the composition over which it is stable exists over a solid solution range, which becomes broader with increasing temperature. The magnesium aluminate spinel can be expressed by the formulation $MgO{\cdot}nAl_2O_3$ [10], in which n ranges from 0.8 (MgO-rich) to 3.5 (Al_2O_3-rich) at appropriate temperatures [10,11].

The magnesium-doped α-alumina shows good proton conduction at high temperature [12,13]. Also, it is known that Mg-Al spinel can replace the conventionally-used Al_2O_3, as a substrate for GaN growth [14]. The Mg-Al spinel exhibits a favorable combination of physical and chemical properties. Since the cleavage direction of stoichiometric spinel ($MgAl_2O_4$, $MgO{\cdot}nAl_2O_3$ with n=1), the [110] direction, is parallel to the cleavage direction of wurtzite GaN, which is the [1120] direction, device fabrication process will become simpler. In particular, alumina-rich spinel ($Mg_{0.4}Al_{2.4}O_4$, $MgO{\cdot}nAl_2O_3$ with n=3; 1:3 spinel), can be easily sliced and polished into large-diameter wafers, due to the compositional softening. Furthermore, the 1:3 spinel is favorable for the crystal growth, due to its lower growth temperature.

Recently, in order to create potential applications and to introduce peculiar properties, further modification and variation of the morphology and structure of 1D nanomaterials have been intensively studied. For example, branched nanostructures have attracted interest because they help to achieve parallel connectivity and interconnection of different functional elements [15].

In the present study, in order to explore the novel structures and properties, a mixture of Mg and Al powders was thermally heated at various temperatures and novel-structured materials composed of MgO backbone nanowires and donut-shaped spinel structures were prepared at 1,000 ℃. The arrays of disc-or donut-typed nanostructures obtained in this study can be utilized as a mixture or as an individual functional material if one component is selectively removed. Furthermore, a combination of dissimilar materials will generate more peculiar and useful properties.

We revealed that the substrate temperature affected the growth mechanisms. The high-temperature process facilitates the tip-growth process and thus the generation of a mixture of particles. This novel material is completely different from

*Corresponding author: sangsub@inha.ac.kr, hyounwoo@hanyang.ac.kr

the products of previous vapor-liquid-solid (VLS) processes, in which unnecessary and harmful metal catalytic particles were attached to the nanowire tips. A growth mechanism based on the thermochemical consideration is proposed. The use of the present technology provides a novel route for the growth of novel nanocomposites for commercial production.

2. EXPERIMENTAL PROCEDURES

A mixture of Mg and Al powders was used as a source material with a weight ratio of 1:1 and the powders were fully mixed prior to their use. The synthesis was carried out in a horizontal quartz tube furnace. The mixed powders were located in a ceramic boat, which was subsequently put into a horizontal quartz tube. An Au-coated (Au thickness = 3 nm) Si plate was then placed on top of the ceramic boat, serving as a substrate for collecting the growth products. In order to investigate the effects of temperature, the substrate temperature was set in a range of 950-1,050 ℃. In the growth process, ambient gas with the flow rates of O_2 and Ar being 20 and 100 sccm, respectively, flowed continuously for 1 h.

The products were characterized by glancing angle (0.5°) X-ray diffraction (XRD, X'pert MPD-Philips with $CuK\alpha_1$ radiation) at KBSI, scanning electron microscopy (SEM, Hitachi S-4200), transmission electron microscopy (TEM, Philips CM-200), and energy-dispersive X-ray (EDX) spectroscopy attached to the TEM instrument.

3. RESULTS AND DISCUSSION

Figures 1(a)-(c) show SEM images of the products grown at 950, 1,000, and 1,050℃, respectively, indicating that they are composed of 1D structures. It is noteworthy that 1,000 ℃-grown nanowires exhibit a rough surface. Close examination of the inset reveals that there exist arrays of disc-typed or donut-typed nanostructures on the nanowires. On the other hand, the nanowires produced at 950 and 1,050 ℃ do not have such a peculiar structure, instead revealing the straight-line morphology. Furthermore, there is no catalytic particle on the ends of the nanowires.

Figures 2(a)-(c) show XRD patterns of the products grown at 950, 1,000, and 1,050 ℃, respectively. XRD spectrum for the sample grown at 950 ℃ is comprised of diffraction peaks with respect to cubic MgO (JCPDS: 45-0946) with lattice constants a=0.4211 nm, with some Au and Si peaks from the substrate (Fig. 2(a)). The XRD spectrum of the 1,000 ℃-grown product is almost similar to that of 950 ℃-grown one. However, it is noteworthy that there exists a weak peak, which can be indexed to cubic $(Mg_{0.4}Al_{0.6})Al_{1.8}O_4$ with lattice constants comparable to the values of JCPDS 87-0345. The spectrum of 1,050 ℃-grown product is comprised of a variety of phases. Apart from Si and Au-related peaks, diffraction peaks can be indexed to cubic MgO (JCPDS: 45-0946), cubic $(Mg_{0.4}Al_{0.6})Al_{1.8}O_4$ (JCPDS 87-0345), or cubic $Mg_{0.36}Al_{2.44}O_4$ with a lattice constant of a=0.8975 nm (JCPDS: 77-0729).

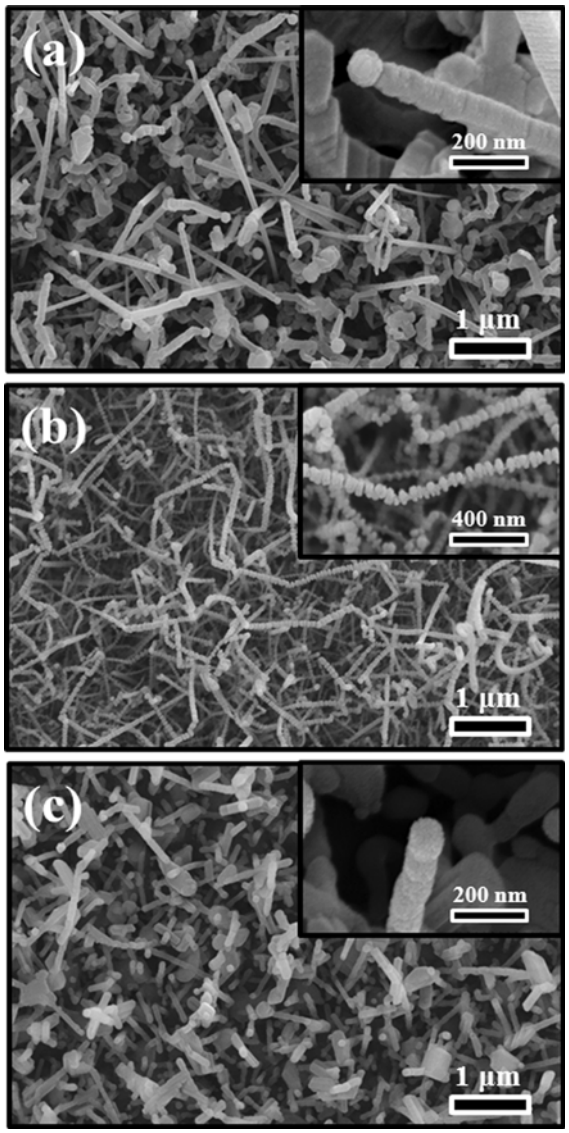

Fig. 1. SEM images of products grown at (a) 950 ℃, (b) 1,000 ℃, and (c) 1,050 ℃ (Inset: Enlarged SEM image).

We have investigated the microstructure of the 1,000 ℃-grown nanowires by means of TEM. Figure 3(a) shows a low-magnification TEM image, indicating that the donut- or disc-shaped nanostructures have been formed. Figure 3(b) shows a typical SAED pattern. The well-defined SAED pattern clearly shows diffraction spots, corresponding to the (020), (002), and (022) lattice planes of cubic MgO. In addition, the SAED pattern exhibits relatively weak diffraction spots corresponding to the (022) and $(0\bar{2}2)$ lattice planes of cubic $(Mg_{0.4}Al_{0.6})Al_{1.8}O_4$. Herein, the corresponding SAED pattern can be indexed as a superimposition of those from MgO and $(Mg_{0.4}Al_{0.6})Al_{1.8}O_4$ in the [001] pole direction. The epitaxial relationship is determined to be $(001)_M \parallel (001)_S$ and

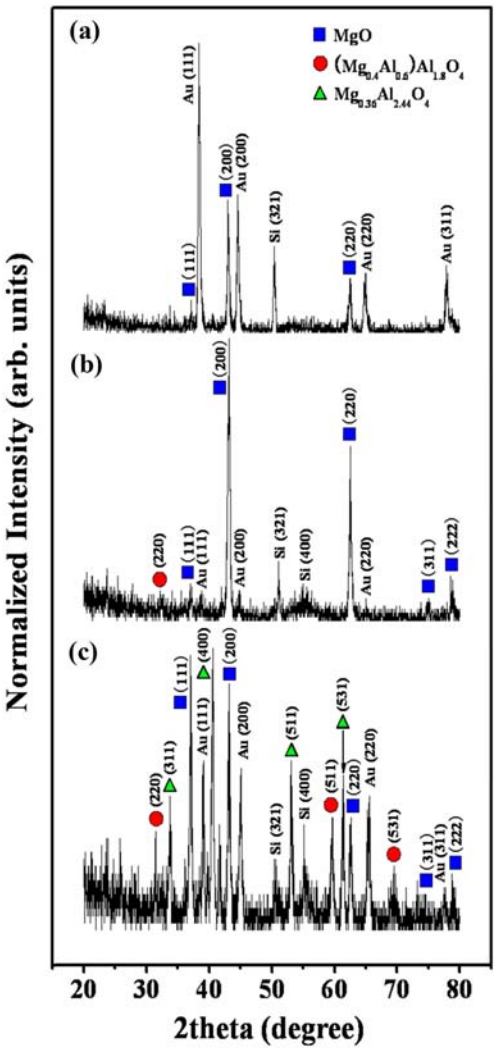

Fig. 2. XRD patterns of products grown at (a) 950 °C, (b) 1,000 °C, and (c) 1,050 °C.

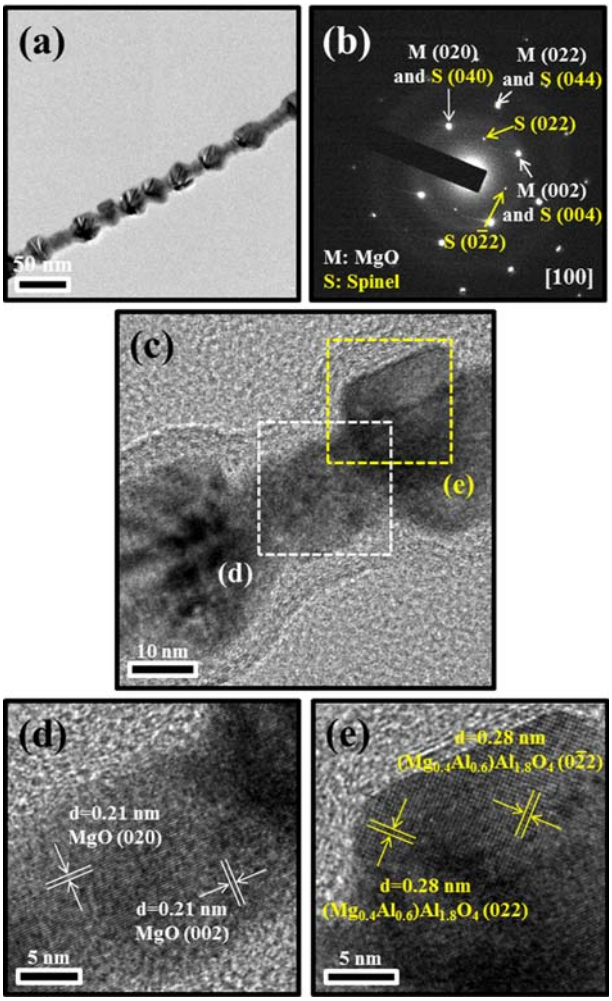

Fig. 3. (a) Low-magnification TEM image of a 1,000 °C-grown nanowire. (b) Typical SAED pattern. (c) Enlarged TEM image exhibiting the donut-shaped nanostructures. (d,e) Lattice-resolved TEM images of the boxed regions in (c).

$(100)_M \parallel (100)_S$ (the subscripts M and S denote MgO and spinel, respectively). Similar epitaxial relations were reported for $MgO/MgAl_2O_4$ [16] and MgO/Mg_2TiO_4 [17].

In order to investigate the donut-shaped structure, we have employed the lattice-resolved TEM image. Figure 3(c) is an enlarged TEM image, clearly exhibiting that the donut-shaped structures surround the nanowires. Figures 3(d) and 3(e) show the lattice-resolved TEM images of the boxed regions in Fig. 3(c). Figure 3(d) shows a crystalline structure with observable lattice spacings of approximately 0.21 nm, which correspond to the {200} planes of cubic MgO. On the other hand, Figure 3(e) shows the lattice fringes corresponding to the (022) and (0$\bar{2}$2) lattice planes of cubic $(Mg_{0.4}Al_{0.6})Al_{1.8}O_4$.

For comparison, we have carried out TEM for the 1,050 °C-grown nanowires. Figure 4(a) shows a low-magnification TEM image, indicating that the surface of the nanowire is relatively smooth. Figure 4(b) shows the corresponding SAED pattern recorded perpendicular to the rod axis, as it was indexed for the [1$\bar{1}$0] axis of crystalline $(Mg_{0.4}Al_{0.6})Al_{1.8}O_4$. The pattern reveals the presence of diffraction spots, corresponding to the (002), (111), and (220) lattice planes of cubic $(Mg_{0.4}Al_{0.6})Al_{1.8}O_4$. Figure 4(c) shows the lattice-resolved TEM image, which enlarges the boxed region in Fig. 4(a). It exhibits the fringes corresponding to the (220), (002), and (111) lattice planes of cubic $(Mg_{0.4}Al_{0.6})Al_{1.8}O_4$.

In the present study, we revealed that the growth temperature played a crucial role in determining the phase and structure of the 1D nanostructures. (i) Pure MgO nanowires have been produced at a temperature of 950 °C. (ii) Peculiar nanowires with surrounded donut-like nanostructures, were produced at 1,000 °C. The "nanodonuts" were comprised of an alumina-rich spinel phase, whereas the backbone nanowire an MgO phase. (iii) alumina-rich spinel nanowires were produced at 1,050 °C. From the phase diagram of the MgO-

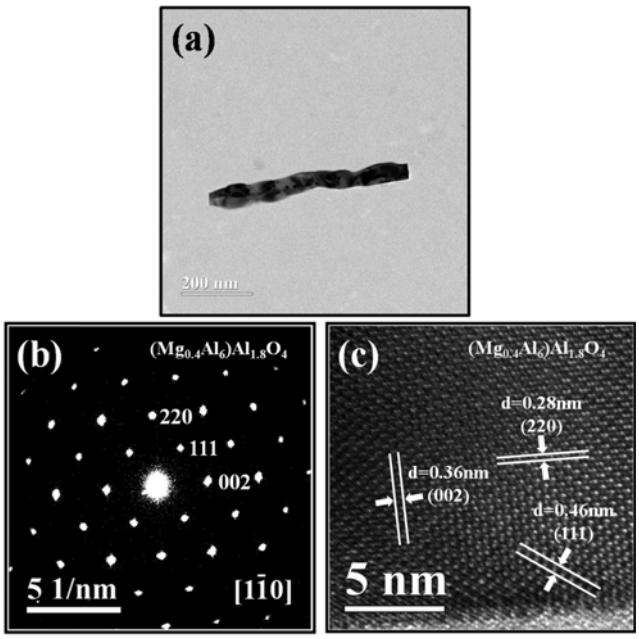

Fig. 4. (a) Low-magnification TEM image of a 1,050 °C-grown nanowire. (b) Typical SAED pattern. (c) Lattice-resolved TEM images of the boxed regions in (a).

Al_2O_3 system [18], it is clearly expected that the MgO and spinel phases coexist in the MgO-sided section, whereas the Al_2O_3 and spinel phases coexist in the Al_2O_3-sided section. Furthermore, it was observed that no spinel but pure MgO nanowires have been produced at 950 °C. Accordingly, the overall composition of the product lies in the MgO-sided section of the phase diagram. From the diagram, we know that the spinel phase should be included in the product. However, the absence of the spinel structure in the MgO nanowires at 950 °C, but the reappearance at 1,000 and 1,050 °C are against the phase diagram. We suspect that nucleation kinetics may play a role in the present experiment. We simulated the experiment by using a mixture of Al (45 g), Mg (45 g) and Si (10 g), where the 10 g of Si was used to represent the fact that the applied silicon substrate may be involved in the chemical reaction. By using a commercial thermochemistry software FactSage, the above mixture was found to be in the equilibrium state of liquid and Mg_2Si (solid) at 945 °C, whereas it was in a pure liquid state at temperatures higher than 945 °C owing to the melting of Mg_2Si phase. The following reaction was used: 45g Mg + 45g Al + 10g Si = 99.94 g liquid phase + 0.06g Mg2Si. Herein, the liquid phase composition is: 45.03 wt%Al, 44.99 wt%Mg and 9.98 wt% Si. Although the thermochemical data shown below reveal that the Mg_2Si structure is stable as a solid phase up to the temperature of 1100 °C in pure Si-Mg system [19], the solid Mg2Si will appear at 945 °C in ternary Si-Mg-Al system. It is reasonable to speculate that Mg_2Si serves as nucleation sites for MgO when the system is exposed to oxygen. Without the formation of Mg_2Si at 1,000 °C, spinel has a fair chance to form along with the less aggressive MgO in this two-phase equilibrium zone. Accordingly, at 1000 °C, not only spinel but also MgO phase will be formed. At 1,050 °C no MgO but spinel is formed, therefore, the transition temperature of two-phase-system (MgO + spinel) to one-phase-system (spinel) is located between 1,000 to 1,050 °C. The XRD observation indicates that the 1,050 °C-grown product is comprised of a variety of phases, including MgO, $(Mg_{0.4}Al_{0.6})Al_{1.8}O_4$, and $Mg_{0.36}Al_{2.44}O_4$. However, TEM observation indicates that the 1,050 °C-grown product is mainly comprised of alumina-rich spinel nanowires. Accordingly, it is possible that MgO and $Mg_{0.36}Al_{2.44}O_4$ structures are mainly deposited on the substrate presumably in the form of clusters or films, whereas $(Mg_{0.4}Al_{0.6})Al_{1.8}O_4$ structure has predominantly been grown in a wire form. The temperature-dependent evaporation behavior of Al powder thus explains why MgO and alumina-rich spinel nanowires were predominantly obtained at low (950 °C) and high (1,050 °C) temperatures, respectively. Using the XRD patterns, the lattice parameters can be calculated: Lattice parameter of MgO nanowires grown at 950 °C is 4.202Å, that of MgO cores grown at 1,000 °C is 4.183Å. The core MgO has a smaller lattice parameter than MgO nanowires that have a similar one to a single crystal (4.211Å). An explanation for the reduced lattice parameter at 1,000 °C is that the solubility of Al_2O_3 in MgO is higher at 1,000 °C than 950 °C. Substitution of Mg by Al in the MgO solid solution may reduce the lattice parameter.

In order to investigate the chemical composition of the whiskers grown at 1,000 °C, we carried out an EDX analysis. Although it is not shown in the present paper, electron mapping analysis reveals that the nanowire is comprised of Mg, Al, and O elements. In addition, Figure 5(a) shows a

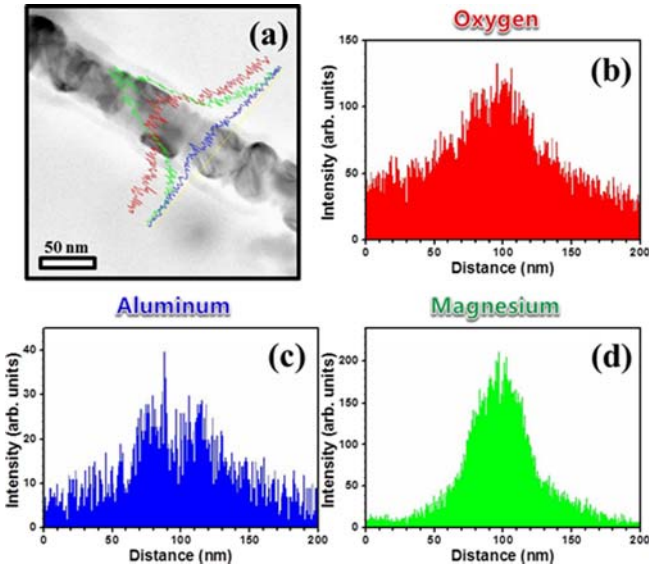

Fig. 5. (a) TEM image of a 1,000 °C-grown nanowire and corresponding EDX line scans along the nanodonut-decorated region of the nanowire, in regard to (b) O, (c) Mg, and (d) Al elements.

typical nanodonut-decorated nanowire grown at 1,000 °C. As shown in Figure 5(a), the composite nanowire is comprised of bare and spinel-nanodonut-decorated regions. Figures 5(b)-(d) show the concentration profiles of O, Al, Mg elements, across the nanowire diameter in Fig. 5(a). The concentration of Mg and O elements become maximized at the center of the nanowire, which can be understood by considering the circular cross-section of the nanowire. In addition, it is noteworthy that the concentration profile of Al is valley-like, in which the highest peaks are in the shell region (Fig. 5(c)).

By the way, it is noteworthy that a slight increase of growth temperature results in the fabrication of spinel-nanodonut-decorated MgO nanowires (Fig. 6). Although it is expected that the high temperature spinel phase will appear at 1,000 °C, it is unclear why the donut-shaped spinel structure surrounded the core MgO nanowires. However, we speculate that the strain established between the core MgO nanowire and the surrounded spinel is likely to be responsible for the creation of the periodic donut-shaped spinel shell. At early stages of growth, the spinel phase starts to grow on the core MgO nanowire, likely forming core-shell nanowires. The generation of spinel phase can be processed by the diffusion process. Since this MgO nanowires surrounded by a donut-shaped spinel, produced in the present work, is the exceptionally peculiar structure, which has never been reported. Therefore, it is very difficult to reveal the detailed mechanism. However, it is possible that the formation of nanodisks at 1000 °C is the result of the diffusion-controlled phase separation. For example, from the phase diagram of MgO-Al_2O_3 (without considering Si phase), in the (MgO + spinel) region, MgO and spinel phases become separated below a sufficiently high temperature [18]. At 1000 °C, it is possible that MgO will start to grow from liquid. Subsequently, the spinel structure will be grown from the remaining liquid or from the solid MgO structure. This spinel growth can be controlled by diffusion process.

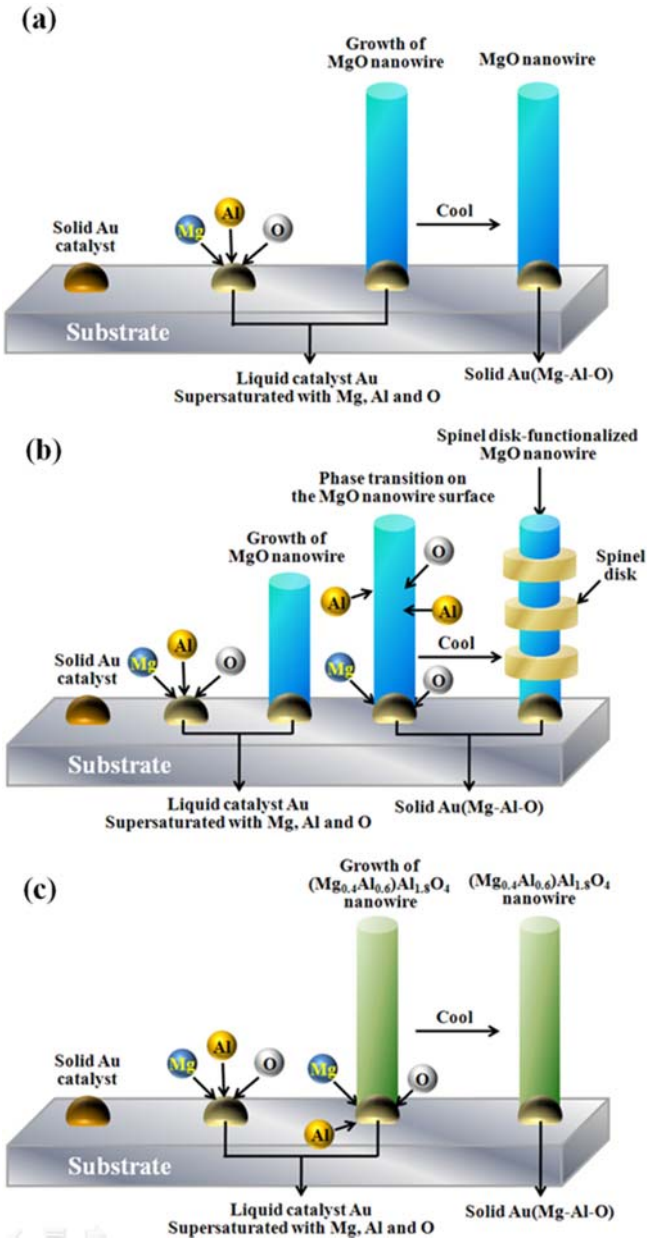

Fig. 6. Schematic illustration of the growth mechanism of the whiskers grown at (a) 950 °C, (b) 1,000 °C, and (c) 1,050 °C.

The continuous spinel shell will experience a considerable strain, which is the driving source of the periodically-separated disk-shaped spinel shell in which the strain can mostly be relieved. Using the XRD patterns in Fig. 2, the lattice parameters could be calculated: Lattice parameter of MgO nanowires grown at 950 °C was 4.202 Å, while that of MgO cores with the spinel being surrounded grown at 1,000 °C was 4.183 Å. The difference of the lattice parameter is negligible, which obviously demonstrates the sufficient strain release.

Up to the present, a large number of various 1D structures have been synthesized, and there are two well-accepted growth mechanisms of 1D structures: the vapor-solid-liquid (VLS) and the vapor-solid (VS) mechanisms. Based on the observation that there exists no particle being attached to the tips of the whiskers, we conclude that the growth of 1D nanowires in the present study is mainly controlled by a VS process. With a mixture of Mg and Al powders being evaporated with oxygen, which was supplied from the carrier gas, Au/Mg/Al/O liquid droplets are formed on the substrate, presumably because the growth temperature exceeds the eutectic temperature. At the low temperature of 950 °C, however, the evaporation of Al powder will be relatively negligible, forming the Au/Mg/O liquid droplets.

The spinel-donuts-surrounded MgO nanowires have the following potentials. First, they can be used with respect to the strain engineering: $MgAl_2O_4$ is strained by MgO, which will influence the band structure of $MgAl_2O_4$ [20]. Second, they have potential in regard to the magnet resistivity or spintronics. For example, monocrystalline $MgAl_2O_4$ barrier was used for

magnetic tunnel junctions and exhibited an excellent spin-transfer magnetization switching behavior, in comparison to the MgO barrier [21]. Accordingly, with the use of the spinel-donuts-surrounded MgO backbone nanowires, the switching behavior can be controlled in a wide range from MgO to spinel by modulating the periodicity of spinel donuts.

With a significant amount of studies on nanostructures having been previously reported [22-32], the present work can be a cornerstone for the future applications of nanostructures.

4. CONCLUSIONS

We have heated a mixture of Mg and Al powders at temperatures in the range of 950-1,050 ℃. We reveal that the growth temperature affected the structure and morphology of the produced 1D nanowires. We have characterized samples by means of SEM, TEM, SAED, and XRD. SEM investigation reveals that the 1,000 ℃-grown nanowires have a peculiar morphology with arrays of disc-or donut-typed nanostructures. We have conducted the TEM investigation in terms of SAED pattern and lattice-resolved TEM image, revealing that the 1,000 ℃-grown product exhibits a very extraordinary morphology, with the donut-shaped spinel structure surrounding the core MgO nanowires. On the other hand, both 950 ℃- and 1,050 ℃-grown ones corresponded to the normal nanowires. The 950 ℃-grown nanowires correspond to a pure cubic MgO structure, whereas the 1,050ºC-grown ones are comprised of cubic $(Mg_{0.4}Al_{0.6})Al_{1.8}O_4$ phase. From the absence of tip nanoparticles, we reveal that the synthesis of nanowires in the present study is dominated by a base-growth process. By means of the thermochemistry calculations, we propose that the absence of spinel in samples equilibrated at 950 ℃ resulted from the catalyst-like behaviors of the silicon substrate, facilitating the formation of MgO.

ACKNOWLEDGEMENTS

This work was supported by the National Research Foundation of Korea (NRF) grant funded by the Korea government (MEST) (No. NRF-2013R1A2A2A01068438).

REFERENCES

1. A. F. Dericioglu and Y. Kagawa, *J. Eur. Ceram. Soc.* **23**, 951 (2003).
2. M. Shimada, T. Endo, T. Saito, and T. Sato, *Mater. Lett.* **28**, 413 (1996).
3. G. C. Wei, *J. Phys. D: Appl. Phys.* **17**, 3057 (2005).
4. J. Guo, H. Lou, H. Zhao, D. Chai, and X. Zheng, *Appl. Catal. A:Gen.* **273**, 75 (2004).
5. J. Guo, H. Lou, H. Zhao, X. Wang, and X. Zheng, *Mater. Lett.* **58**, 1920 (2004).
6. M. Beauvy, C. Dalmasso, C. Thiriet-Dodane, D. Simeone, and D. Gosset, *Nucl. Instrum. Meth. Phys. Res. B* **242**, 557 (2006).
7. M. C. L. Patterson, A. A. DiGiovanni, D. W. Roy, and G. Glide, *Ceram. Transact.* **151**, 83 (2003).
8. G. Gusmano, G. Montesperelli, E. Traversa, A. Bearzotti, G. Petrocco, A. D'Amicon, and C. Di Natale, *Sens. Actuators B* **7**, 460 (1992).
9. S. Mukhopadhyay, S. Ghosh, M. K. Mahapatra, R. Mazumder, P. Barick, S. Gupta, and S. Chakraborty, *Ceram. Int.* **28**, 719 (2002).
10. A. C. Sutorik, G. Gilde, C. Cooper, J. Wright, and C. Hilton, *J. Am. Ceram. Soc.* **95**, 1807 (2012).
11. E. F. Osborn, *J. Am. Ceram. Soc.* **36**, 147 (1953).
12. N. Fukatsu, N. Kurita, Y. Oka, and S. Yamamoto, *Solid State Ionics* **162**, 147 (2003).
13. N. Kurita, N. Fukatu, N. Miyasmoto, M. Takada, J. Hara, M. Kato, and T. Ohashi, *Solid State Ionics* **162**, 135 (2003).
14. H. Tang, J. Xu, H. Li, Y. Dong, F. Wu, and M. Chen, *J. Alloys Compd.* **479**, L26 (2009).
15. Q. Wan, J. Huang, Z. Xie, T. Wang, E. N. Dattoli, and W. Lu, *Appl. Phys. Lett.* **92**, 102101 (2008).
16. H. Fan, M. Knez, R. Scholz, K. Nielsch, E. Pippel, D. Hesse, U. Gösele, and M. Zacharias, *Nanotechnology* **17**, 5157 (2006).
17. D. Hesse and H. Bethge, *J. Cryst. Growth* **52**, 875 (1981).
18. T. I. Barry, A. T. Dinsdale, J. A. Gisby, B. Hallstedt, B. Jansson, S. Jonsson, B. Sundman, and J. R. Taylor, *J. Phase Equil.* **13**, 459 (1992).
19. I. Barin, *Thermochemical Data of Pure Substances, 3rd ed.*, p. 1029, VCH Publishers, Inc., New York, NY (USA) (1995).
20. K. C. George, S. Kurien, and J. Mathew, *J. Nanosci. Nanotech.* **7**, 2016 (2007).
21. H. Sukegawa, S. Mitani, T. Ohkubo, K. Inomata, and K. Hono, *Appl. Phys. Lett.* **103**, 142409 (2013).
22. S. J. Yoo and W. J. Kim, *Korean J. Met. Mater.* **52**, 561 (2014).
23. C.-H. Lim, H.-S. Kim, Y.-T. Yu, and J.-S. Park, *Met. Mater. Int.* **20**, 323 (2014).
24. H. Ghasemi-Nanesa, M. Nili-Ahmadabadi, A. Mirsepasi, and C. Zamani, *Met. Mater. Int.* **20**, 201 (2014).
25. M. R. Vaezi and A. Esmaielzadeh Kandjani, *J. Ceram. Proc. Res.* **15**, 376 (2014).
26. M. Badr-Mohammadi, I. Mobasherpour, E. Marzban Rad, and G. Mortazavi, *J. Ceram. Proc. Res.* **15**, 88 (2014).
27. N. Zhang, T. Fu, F. Yang, H. Kan, X. Wang, H. Long, and L. Wang, *J. Ceram. Proc. Res.* **15**, 93 (2014).
28. L. Han, L. Zheng, Z. Hu, S, Yin, and Y. Zeng, *Electron. Mater. Lett.* **10**, 1 (2014).
29. Sh. Valedbagi, J. Jalilian, S. M. Elahi, S. Majidi, A. Fathalian, and V. Dalouji, *Electron. Mater. Lett.* **10**, 5 (2014).
30. M. S. Kale, Y. R. Toda, M. P. Bhole, and D. S. Bhavsar, *Electron. Mater. Lett.* **10**, 21 (2014).
31. S. Chawl, M. Saroha, and R. K. Kotnala, *Electron. Mater. Lett.* **10**, 73 (2014).
32. M. Khajelakzay and E. Taheri-Nassaj, *Electron. Mater. Lett.* **10**, 117 (2014).